

Physically-Based Simulation of Electromigration Induced Failures in Copper Dual-Damascene Interconnect

Valeriy Sukharev

LSI Logic Corporation
1621 Barber Lane, Milpitas, CA 95035 USA
vsukhare@lsil.com

Abstract

We have developed a novel physical model and a simulation algorithm capable of predicting electromigration (EM) induced void nucleation and growth in an arbitrary interconnect segment. Incorporation of all important atom migration causes into the mass balance equation and its solution together with solution of the corresponding electromagnetics, heat transfer and elasticity problems, in a coupled manner, has provided a capability for the EM design rules generation/optimization with the physically based simulations. As an example, we have demonstrated the model capability to discriminate an early failure from a long term one taking place in a via containing copper dual damascene (DD) structure.

1. Introduction

Implementation of copper and low-K materials as major components of interconnect structures has resulted in the necessity to create new physical and electrical current design rules to ensure chip immunity to EM-induced failures. This practical demand necessitates an enormous interest in understanding the fundamental reliability properties of copper dual-damascene metallization. Physically based models and simulations can be considered as powerful tools that can help address this demand. Implementation of reliability simulation capabilities at the design rules generation step can help avoid an unnecessary conservative approach, which reduces possible chip performance. To be able to reach this target a comprehensive simulation model of metal migration-induced failure should be employed. In the general case, detailed 3-D modeling should be applied. This is especially true for copper metallization characterized by a complicated geometry of the DD interconnect segments and by much lower critical stress for void nucleation than aluminum. The latter fact clarifies an important role of non-uniform stress, current and temperature distributions in failure development. Numerous experimental data and a number of theoretical results have created a basis for

understanding of the major mechanisms governing the reliability of the Cu interconnect [1]. The problem that was not addressed yet is the availability of the practical and robust simulation model capable of capturing these major mechanisms of failure. Such model should be employed for optimization of the interconnect design in order to increase its lifetime.

The coupled multiphysics character of the EM phenomenon is a problem that causes enormous difficulties with a priori prediction of the exact location of EM induced void nucleation and the major direction of its growth in an arbitrary interconnect segment. Indeed, atom migration caused by a combination of driving forces working together can generate voids in different locations depending on interrelations between the driving forces. These forces result from different physical causes such as momentum exchange with current carriers (electron wind), gradients in atom concentration, temperature and mechanical stress [1]. These gradients are responsible for diffusion, thermal diffusion and stress driven diffusion correspondingly. In general, atom redistribution, caused by an applied electrical current, generates gradients in atom density and mechanical stress which, working against electrical current action, tend to bring the atomic system to equilibrium. Depending on the particular segment geometry, interconnect material properties and applied electrical current, either the mentioned equilibrium can be achieved or a void can be nucleated somewhere in the interconnect segment. The fact of void nucleation indicates that the tensile stress, generated somewhere in the segment area with depleted atom concentration, has reached a critical level and was relaxed by void formation. The nucleated void affects the current density, temperature and mechanical stress distributions in the void vicinity and, hence, changes the local atomic fluxes in the area surrounding the void. Depending on the system geometry, material properties and current density as well as on interaction between voids in the case of multi void nucleation, the particular void either grows or disappears. Kinetics of void evolution is governed again by the total atomic flux generated by all considered driving forces. This already complex picture of atom migration induced void

nucleation and growth becomes even more complicated with introduction of a grain structure and corresponding fast diffusion paths, associated with grain boundaries and interconnect interfaces [1-3].

In this study we have developed and solved a transient, fully linked EM model. The developed model targets void nucleation and its growth kinetics as a function of the segment geometry, interconnect architecture and electrical loading. We took into consideration all important atom migration causes: electron induced momentum transfer, time-dependent stress gradient, thermal diffusion, and concentration gradient. Implementation of a vacancy based diffusion mechanism [4,5] has provided us with the capability to accurately implement stress dependent atom diffusivity, which is different in different regions of the interconnect segment. Coupling of the electromagnetics, heat transfer, structural mechanics and atom migration models, based on direct solution of a system of partial differential equations using the finite element method (FEM) [6], has allowed us to simulate stress-induced void nucleation and growth in different interconnect segments.

2. Model

Full EM modeling should take into consideration all possible driving forces for atom migration such as (i) momentum transfer between the electric current carriers and the atoms of a conducting medium, (ii) mechanical stress gradients existing in the conductor before an electric current is applied, as well as developed by the atom density redistribution inside the conductor embedded into a rigid confinement, (iii) a temperature gradient existing inside the conductor, and, finally, (iv) an atom concentration gradient developed by the atom redistribution. All these forces should be simultaneously and self-consistently taken into account in the EM model in order to adequately describe the continuous atom redistribution [7-14]. This redistribution of the atom density results in the development of an essential tensile stress in the segment areas, which are characterized by the atom depletion. Tensile stress generation causes the increase in the vacancy concentration that speeds up the rate of reaction of vacancy coalescence, leading to void nucleation. All these phenomena should be implemented into the EM model.

A governing equation, which describes the atom density evolution caused by an applied current, is the traditional mass balance (continuity) equation

$$\frac{\partial N}{\partial t} + \vec{\nabla} \vec{J} = 0, \quad (1)$$

where $N(r, t)$ is the atom concentration at the $r=\{x, y, z\}$ location at the moment of time t , and J is the total atomic flux at this location, which is a combination of the fluxes caused by all above mentioned forces: namely by the electric

current, and by the gradients of temperature, mechanical stress and concentration

$$\vec{J}_C = \frac{NeZD\rho}{kT} \vec{j} \quad (2)$$

$$\vec{J}_T = -\frac{NDQ}{kT^2} \vec{\nabla} T, \quad (3)$$

$$\vec{J}_S = \frac{ND\Omega}{kT} \vec{\nabla} H, \quad (4)$$

$$\vec{J}_N = -D\vec{\nabla} N. \quad (5)$$

Here, e is the electron charge, eZ is the effective charge of the migrating atom, ρ is the resistivity of the conductor, where atom migration takes place, j is the local current density, k is Boltzmann's constant, T is the absolute temperature, Q is the heat of thermal diffusion, $\Omega=1/N_0$ is the atomic volume and N_0 is the initial atomic concentration, $H=(\sigma_1+\sigma_2+\sigma_3)/3$ is the hydrostatic stress, where $\sigma_1, \sigma_2, \sigma_3$ are the components of principal stress, and $D(r, t)$ is the time and position dependent atom diffusivity. Assuming a vacancy mechanism for atom diffusion [4, 5], we can express D as a function of the hydrostatic stress

$$D = D_0 \exp\left\{\frac{\Omega H - E_A}{kT}\right\} \quad (6)$$

where E_A is the effective activation energy of the thermal diffusion of metal atoms. The multiplier $\exp\{\Omega H/kT\}$ comes from the dependency of the vacancy concentration on stress [14]. The vacancy concentration represents availability of empty lattice sites, which might be occupied by a migrating atom.

The total atomic flux can be rewritten on the basis of expressions (2)-(6) as a combination of the diffusion and convection-like fluxes

$$\vec{J} = -D\vec{\nabla} N + \vec{\Phi} N \quad (7)$$

and the mass balance equation takes the form

$$\frac{\partial N}{\partial t} + \vec{\nabla}(-D\vec{\nabla} N + \vec{\Phi} N) = 0, \quad (8)$$

where

$$\vec{\Phi} = \frac{D}{kT} (eZ\vec{j}\rho - \frac{Q}{T} \vec{\nabla} T + \Omega \vec{\nabla} H). \quad (9)$$

Equation (8) describes the atom concentration evolution at any point of the considered segment characterized by the given j, T and gradients of temperature and stress. Thus, to

get a complete solution of the problem we should determine in coupled manner evolution of the current, temperature and stress distributions in the considered segment, caused by continuous atom density redistribution. Assuming, that an almost immediate establishment of a new equilibrium in the current, temperature and stress distributions accompanies slow atom migration, we can employ the steady-state solutions for the current, temperature and stress, obtained for the different atom density distributions. To obtain the kinetics of the atom density evolution in an arbitrary interconnect segment, stressed by the electric current, the mass balance equation (8) should be solved in the coupled manner with the corresponding electromagnetics, heat transfer, and structural mechanics equations. The complete system of equations for all-important variables is formed by Laplace's (10), Fourier's (11), Navier's (12) and mass balance (13) equations:

$$\vec{\nabla}\left(\frac{1}{\rho}\vec{\nabla}V\right)=0, \quad (10)$$

$$-\vec{\nabla}(k_T\vec{\nabla}T)-\frac{(\vec{\nabla}V)^2}{\rho}=0, \quad (11)$$

$$(\mu+G)\frac{\partial\epsilon}{\partial x_i}+G\Delta u_i-\frac{E}{1-2\nu}(\alpha_T\frac{\partial T}{\partial x_i}+\Omega\frac{\partial N}{\partial x_i})=0, \quad (12)$$

$$\frac{\partial N}{\partial t}+\vec{\nabla}(-D\vec{\nabla}N+\frac{DN}{kT}(\Omega\vec{\nabla}H-\frac{Q}{T}\vec{\nabla}T+eZ\vec{\nabla}V))=0, \quad (13)$$

where

$$\rho=\rho_0[1+\beta(T-T_0)]. \quad (14)$$

Here, $\rho_0=\rho(T_0)$, β is the temperature coefficient of resistivity, T_0 is the reference temperature, $x_i=\{x, y, z\}$ are the local coordinates, α_T is the thermal expansion coefficient,

$$\mu=E\frac{\nu}{(1+\nu)(1-2\nu)}, \quad (15)$$

$$G=\frac{E}{2(1+\nu)}, \quad (16)$$

where E is the Young's modulus, ν is Poisson's ratio, and ϵ is the volume expansion

$$\epsilon=\sum_i\frac{\partial u_i}{\partial x_i}, \quad (17)$$

which is related to the hydrostatic stress as

$$H=\frac{E(\epsilon-3\alpha_T\Delta T-3\Omega\Delta N)}{3(1-2\nu)}. \quad (18)$$

Hence, the spatial atom density evolution, caused by the applied electrical current, can be derived from the solution of the system of equations (10)-(18).

The solution of this system of equations, in the form as they are presented above, describes the evolution of all variables of interest for the initial time interval, while voids have not nucleated. Void nucleation should modify the kinetics of all these variables. The traditional approach to capture these modifications in the FEM approach consists of the introduction of a free surface corresponding to the shape and size of the nucleated void, re-meshing the remaining portion of the conductor, and solving the same system of equations [7, 11]. This procedure should be iterated to get continuous kinetics of the void growth and evolution of all variables of interest. This recurring re-meshing followed by coupled multiphysics simulation makes it extremely difficult to reach a converged solution. Another approach to capturing the void nucleation and growth by means of simulations with a FEM code was described by Weide-Zaage and coworkers [15]. This approach deals with modification of the material properties of the portion of conductor occupied by the growing void. The inside void electrical conductivity, thermal conductivity, Young's modulus etc. should be reduced from the values corresponding to the considered metal to almost zero, which corresponds to vacuum. This approach, providing a physically meaningful solution of the problem, avoids enormous numerical difficulties associated with the introduction of free surfaces. For the sake of model simplification we have introduced the threshold atomic concentration N_c , below which a void should be nucleated. In other words, all parts of the conductor characterized by the atom density lower than N_c will be occupied by the expanding void. This condition occurs through relations between atomic concentration, hydrostatic stress and the vacancy concentration. Indeed, if the atom density inside some part of the metal segment is reduced by EM, then a tensile stress is developed in this area. The stress intensity depends on how rigid the confinement is. Thus, low-K ILD will generate smaller stress inside an embedded metal line than the conventional silicon dioxide ILD. The generated tensile stress results in an exponential growth of the vacancy concentration in accordance with the equation

$$N_v=N_{v0}\exp\left\{\frac{\Omega H}{kT}\right\}. \quad (19)$$

This vacancy concentration growth should increase the rate of reaction of coagulation of vacancies, leading to void nucleation. Here, $N_{v0}=N_0\exp\{E_v/kT\}$ is the equilibrium vacancy concentration under zero stress condition; E_v is the activation energy of the vacancy formation.

3. Aluminum-silicon dioxide interconnect

It is already common knowledge that, in the case of Al interconnect, the main channel for atom migration is represented by a network of grain boundaries. It is a well established fact that Al atoms diffuse faster along the grain boundaries than through the Al-SiO₂ and Al-TiN/Ti interfaces and much faster than through the Al grain bulk. Comparison studies of the void nucleation and growth in Al lines characterized by multigranular and bamboo structures have supported this conclusion. Atomic transport through Al line, stressed by applied electrical current, can be described qualitatively by the simple model. Momentum exchange between conduction electrons and Al atoms creates a preferred orientation in atom migration coincidental with the current direction. Atoms, migrating by means of hops between neighboring vacant lattice sites, finally reach the grain boundaries and accumulate there. A deposition of extra atoms on the grain boundaries disturbs a balance between the bulk and interface atom concentrations and results in a hydrostatic stress generation caused by a dilation effect. It should be noted that a mean stress value, obtained by stress averaging through a big enough portion of conductor, equals zero. This is easy to understand taking into consideration a vacancy mechanism of atom migration. Indeed, a vacancy flux is exactly equal and oppositely directed to an atom flux. As a result, a local compressive stress generated by the atom deposition at the grain interfaces is compensated by a tensile stress generated somewhere at the grain interfaces by the vacancy accumulation. Hence, the electrical current acts as a pump, which supplies the grain boundaries with the extra atoms and forces them to migrate through the grain boundary network in the direction of current. Small-scale variations in atom concentration, temperature and hydrostatic stress create additional driving forces for the grain boundary migration. A large scale variations in an atom concentration and a corresponding hydrostatic stress distribution are generated at the particular locations inside the metal line, which are characterized by a divergence of total atom flux. Cathode and anode edges of the conductor line, separated from the rest of interconnect by the diffusion barrier liners, are the typical examples of such locations. Considering the grain boundary system as a uniform sublattice with a cell size of the order of magnitude of a mean grain size, we model atom transport as a uniform “bulk” migration, characterized by an effective atom diffusivity, similarly to approach employed in the 1-D EmSim model [3]. This effective diffusivity is a combination of bulk (D_B), grain boundary (D_{GB}) and interface (D_{int}) diffusivities weighted with factors depending on ratios between “thickness” (d_i) of the migration channels and the mean grain size (L) and line height (h)

$$D_{eff} = D_B + \frac{d_{GB}}{L} D_{GB} + 2 \frac{d_{int}}{h} D_{int}, \quad (20)$$

where, d_{GB} and d_{int} are the “thickness” of the migration channels associated with the grain boundaries and Al-Ti/TiN interface.

As an example of implementation of the developed formalism let us consider an aluminum meander deposited on a silicon substrate with a thin intermediate SiO₂ layer. Taking place current crowding results in a void nucleation nearby the rounded corner. The time that is required for the nucleation of this type of voids is much longer than the nucleation time for voids located at the cathode end of the meander. The latter voids were nucleated only when stud-type boundary conditions were applied at the cathode end. Voids of both types are shown in Figure 1. In the case of pad-to-pad BC, the only voids located nearby the current crowding area were nucleated. Hence, in the case of stud-to-stud BC, which represents the meander terminated by vias, we can expect bimodal failure statistics, which should be replaced by a single mode one in the case of a pad-type cathode end. The MTTF for the last type of segments

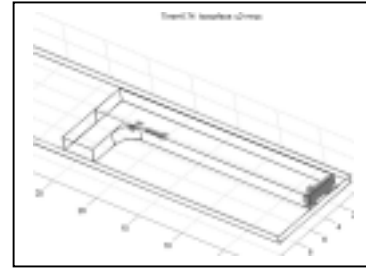


Fig. 1. Void distribution in the meander segment.

will be much longer than for the former. This fact completely corresponds to experiment. It should be noted that we were able to capture both types of voids because of a coupled character of the proposed simulation scheme.

4. Copper – low-K interconnect

The complicated geometry of the interconnect segments created by the DD copper technology demands implementation of the fully linked model for the simulation of EM-induced failure. The presence of a “weak” interface between Cu and an etch stop layer, such as silicon nitride (SiN) or silicon carbide (SiC) [1], should also be taken into account. This interface, while not conducting any electrical current, is characterized nevertheless by faster migration of Cu atoms in comparison with other migration channels such as grain bulks, grain boundaries and interfaces between copper and diffusion barrier liners, for example, Ta/TaN. This asymmetry in distribution of the Cu-atom diffusivity across the cross-section of the Cu-based wire can result in the existence of preferred locations for void nucleation and preferred directions for growth. To be able to capture this behavior we should slightly modify the model described in the previous paragraphs by introduction of the interface

diffusion and atom exchange between the material bulk and interface [16]. Implementation of enhanced interface diffusivity in addition to the “effective” bulk diffusivity

$$D_{eff} = D_B + \frac{d_{GB}}{L} D_{GB}, \quad (21)$$

and introduction of the atom exchange rate between bulk and surface subdomains, which is proportional to the difference between an excessive atom concentration of the bulk atoms ($N-N_0$) and interface atoms concentration M at any point of the interface, makes it possible to get a solution corresponding to the experimental data.

Different Cu-atom diffusivities were introduced for Cu-SiN (D_{SiN}) and Cu-Ta/TaN (D_{TaN}) interfaces in such way that $D_{SiN} > D_{TaN} > D_{GB} \gg D_B$, where D_{TaN} and D_{SiN} are the diffusivities through the Cu/TaN and Cu/SiN interfaces correspondingly. Different atom exchange rates were also introduced between Cu grain bulk and Cu-SiN (Γ_{SiN}) and Cu-Ta/TaN (Γ_{TaN}) interfaces: $\Gamma_{SiN} > \Gamma_{TaN}$. Considering these interfaces as major channels for atom migration we assumed that dilation, associated with the Cu atoms deposition on these interfaces, is a primary cause for the hydrostatic stress development (in addition to the originally developed hydrostatic stress by the cooling a sample down to T_{test} from T_{ref}). The system of equations (10) - (13) should be modified to take into account these model changes. Navier’s equation (12) takes different form in the interface and Cu subdomains

$$(\mu + G) \frac{\partial \varepsilon}{\partial x_i} + G \Delta u_i - \frac{E}{1-2\nu} (\alpha_T \frac{\partial T}{\partial x_i} + \frac{\partial M}{\partial x_i}) = 0, \quad (22)$$

$$(\mu + G) \frac{\partial \varepsilon}{\partial x_i} + G \Delta u_i - \frac{E}{1-2\nu} \alpha_T \frac{\partial T}{\partial x_i} = 0, \quad (23)$$

Mass balance equations for these subdomains are:

$$\frac{\partial M}{\partial t} + \bar{\nabla} \cdot (-D_{int} \bar{\nabla} M + \frac{D_{int} M}{kT} (\Omega \bar{\nabla} H - \frac{Q}{T} \bar{\nabla} T)) = 0, \quad (24)$$

$$\frac{\partial N}{\partial t} + \bar{\nabla} \cdot (-D \bar{\nabla} N + \frac{DN}{kT} (\Omega \bar{\nabla} H - \frac{Q}{T} \bar{\nabla} T + e Z \bar{\nabla} V)) = 0, \quad (25)$$

where, $D_{int} = D_{SiN}$ on the Cu-SiN(C) interface and $D_{int} = D_{TaN}$ on the Cu-TaN interface. Here, $N(x,y,z,t)$ is the “effective” concentration of the Cu atoms inside metal line and $M(x,y,z,t)$ is its concentration at the interfaces.

Implementation of this model into our simulation scheme provides the following picture for void evolution in the case of DD via segment (Figure 2). It can be seen from these pictures that the void is nucleated initially, in accordance with the available experimental data [1,17], at the top left corner of the segment (2,a) and grows along the Cu line and down toward the via. Much later a new void is nucleated at the via bottom (2,b) and grows upward through the via bulk

(2,c-d). Later, these two void coalesce, forming one big void (2,e), which depletes this via completely (2,f) and extends further toward the anode end of the line. It should be noted that the results shown in Fig. 2 have been obtained by solution of the discussed above system of equations (10)-(11) and (22)-(25) when only the electrical current and concentration gradient induced atom fluxes were taken into consideration. Incorporation of the hydrostatic stress gradient induced flux did not change the qualitative character of the

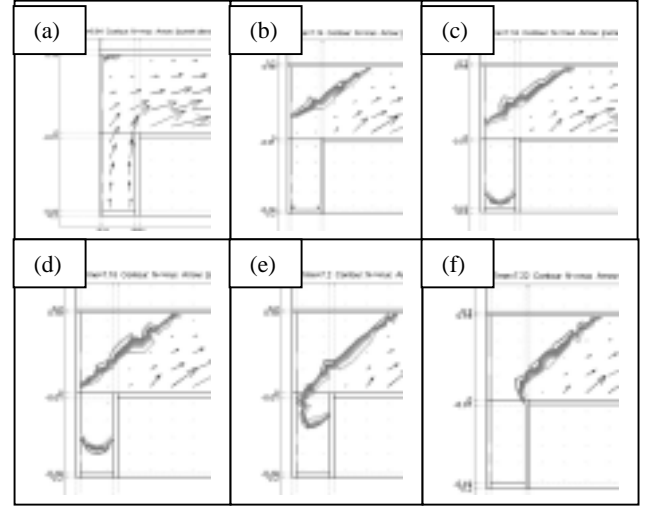


Fig. 2. Void evolution in the DD Cu via segment.

void evolution. The last fact can be explained by the character of hydrostatic stress distribution in the DD via containing segment. It was shown that the existing stress gradient provides an atomic flux toward the Cu-SiN(C) and Cu-Ti/TiN interfaces, in addition to the flux caused by the electrical current. It can be seen from Figures 2,c-f that a continuous void extension takes place even with the depleted via. This is possible if the current can pass through the conductive liners (Fig. 3). Simulation results demonstrate that the character of void evolution strongly depends on the liner conductivity. If this conductivity is very low, then the void nucleates first at the via bottom. The lower the liner conductivity the faster bottom void nucleation happens. Simulation shows that the bottom void, which was nucleated very quickly upon applying an electrical load, was reduced and finally disappeared with the duration of time. Concentration gradient induced atomic flux has resulted in this void recovery. Recovery time depends on the ratio between the current induced flux and diffusion flux. With a larger ratio, a longer healing time can be expected. Such type of void evolution is possible when liners are characterized by small but non-zero conductivity. In the opposite case, the void evolution will stop when it occupies all via bottom interface, undercutting the current inlet.

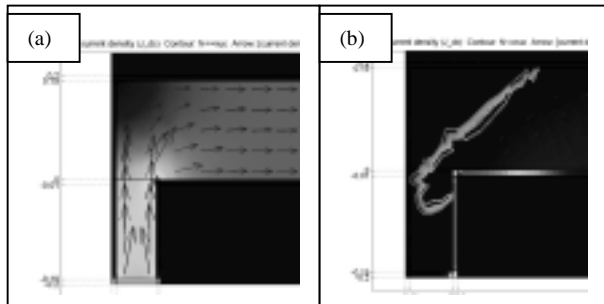


Fig. 3. Current density in the DD Cu via segment before void was nucleated (a) and when via was almost depleted (b).

In the case of high conductive liners these early stage voids do not nucleate at via bottom at all. Increase in copper resistivity, taking place with the depletion in the Cu concentration that we have incorporated in our model and explained by the vacancy-induced scattering, results in redirection of the electrical current through the via liners. This reduction in the electrical current density passing through the via bottom prevents void nucleation. These results can explain the nature of experimentally observed early and long-term failures taking place in the via-containing interconnect segments. Fig. 4 is an example demonstrating a fit between the simulation results and available experimental data in the case of earlier failure.

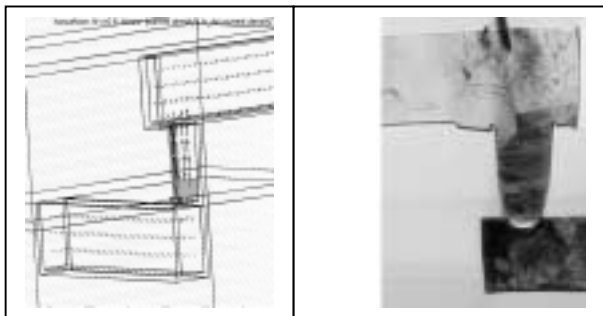


Fig. 4. Void in the DD structure with the upward electron flow.

5. Conclusion

We have developed a novel physical model and a simulation algorithm capable of predicting electromigration induced void nucleation and growth in an arbitrary interconnect segment. All considered examples demonstrate the ability of the presented simulation model to capture the character of the voiding induced failures developed in the interconnect segments under electrical stressing. These simulation efforts are in progress. But even now, the predicted locations of the void nucleation sites as well as the predicted void dynamics in a variety of interconnect segments fit well to the available experimental data. The

models capability for optimization of physical and electrical design rules is stressed. Varying the feature geometry, segment architecture, material properties and some process parameters users are in a position to generate interconnect with the high immunity to EM-induced failures.

6. References

- [1] C.-K. Hu, L. Gignac, E. Liniger, and R. Rosenberg, J. Electrochem. Soc. **149**, G408 (2002).
- [2] P.S. Ho and T. Kwok, Rep. Prog. Phys., **52**, 301 (1989).
- [3] J.J. Clement, IEEE Trans. Dev. Mat. Reliability, **1**, 33 (2001).
- [4] D.W. Malone and R.E. Hummel, Crit. Rev. Sol. State and Mat. Sci., **22**, 199 (1997).
- [5] Y.-J. Park, V.K. Andleigh, and C.V. Thompson, J. Appl. Phys., **85**, 3546, (1999).
- [6] FEMLAB code, COMSOL, Inc. 8 New England Executive Park, Burlington, MA 01803.
- [7] S. Rzepka, E. Meusel, M.A. Korhonen, and C.-Y. Li, Proc. of the 5th Int. Workshop on Stress Induced Phenomena in Metallization, Stuttgart, Germany (1999).
- [8] W.W. Mullins, Metallurgical and Materials Transactions A, **26A**, 1917 (1995).
- [9] A.C.F. Cocks and S.P.A. Gill, Acta Mater., **44**, 4765 (1996).
- [10] M. Schimschak and J. Krug, Phys. Rev. Let., **80**, 1674 (1998).
- [11] A.F Bower and D. Craft, fatigue and Fracture of Engineering Materials and Structures, **21**, 611 (1998).
- [12] A. Averbuch, M. Israeli, I. Ravve, and I. Yavneh, J. Comput. Phys., **167**, 316 (2001).
- [13] J. Wilkening, Mathematical analysis and numerical simulation of electromigration, Ph.D. thesis, University of California, Berkeley (2002).
- [14] M.A. Korhonen, P. Borgesen, K.N. Tu, and C.-Y. Li, J. Appl. Phys., **73**, 3790, (1993).
- [15] D. Dalleau and K. Weide-Zaage, Microelectronics Reliab., **41**, 1625 (2001).
- [16] R. Rosenberg and M. Ohring, J. Appl. Phys., **42**, 5671 (1971).
- [17] E. Zschech, H. Geisler, I. Zienert, H. Prinz, E. Langer, A.M. Meyer, and G. Schneider, Proc. Advancer Metallization Conference (AMC 2002), MRS, 305 (2002).